

# Cross Section Calculations in Theories of Self-Interacting Dark Matter

Sudhakantha Girmohanta and Robert Shrock

*C. N. Yang Institute for Theoretical Physics and Department of Physics and Astronomy,  
Stony Brook University, Stony Brook, New York 11794, USA*

We study an asymmetric dark matter model with self-interacting dark matter consisting of a Dirac fermion  $\chi$  coupled to a scalar or vector mediator, such that the reaction  $\chi + \chi \rightarrow \chi + \chi$  is well described by perturbation theory. We compute the scattering cross section  $\sigma$ , the transfer cross section  $\sigma_T$ , and the viscosity cross section  $\sigma_V$  for this reaction. As one part of our study, we give analytic and numerical comparisons of results obtained with the inclusion of both  $t$ -channel and  $u$ -channel exchanges and results obtained in an approximation that has often been used in the literature that includes only the  $t$ -channel contribution. The velocity dependences of these cross sections are studied in detail and shown to be in accord with observational data.

## I. INTRODUCTION

There is compelling evidence for dark matter (DM), comprising about 85 % of the matter in the universe. Cold dark matter (CDM) has been shown to account for the observed properties of large-scale structure on distance scales larger than  $\sim 10$  Mpc [1–7]<sup>1 2</sup> (reviews include [8–13].) Some possible problems with fitting observational data on length scales of  $\sim 1–10$  kpc were noticed with early CDM simulations that lacked baryon feedback [14–16]. These included the prediction of greater density in the central region of galaxies than was observed (the core-cusp problem), a greater number of dwarf satellite galaxies than were seen (the missing satellite problem), and the so-called “too big to fail” problem pertaining to star formation in dwarf satellite galaxies. This led to the consideration of models in which dark matter particles have significant self interactions. The extension of cold dark matter  $N$ -body simulations to include baryon feedback can ameliorate these problems with pure CDM simulations [17–28]. Nevertheless, cosmological models with self-interacting dark matter (SIDM) are of considerable interest in their own right and have been the subject of intensive study [14], [29–74]. Other candidates for dark matter, such as primordial black holes [75], mirror dark matter [31, 76, 77], warm dark matter [78–81], ultralight (pseudo)scalar dark matter [82, 83], and dark matter in the context of extra-dimensional models [84, 85] have also been studied but will not be discussed here.

A general estimate shows what size the cross section for scattering of dark matter particles, denoted generically as  $\sigma$ , should be in order to alleviate problems with CDM

simulations lacking baryon feedback. It is necessary that there should be one or more DM-DM scatterings over the age of the universe. The rate of DM-DM scatterings is given by

$$\Gamma = \left( \frac{\sigma}{m_{\text{DM}}} \right) v_{\text{rel}} \rho_{\text{DM}}, \quad (1.1)$$

where  $m_{\text{DM}}$  denotes the mass of the DM particle. Numerically, this is

$$\Gamma = 0.1 \text{ Gyr}^{-1} \left( \frac{\sigma/m_{\text{DM}}}{1 \text{ cm}^2/\text{g}} \right) \left( \frac{v_{\text{rel}}}{50 \text{ km/s}} \right) \left( \frac{\rho_{\text{DM}}}{0.1 M_{\odot}/\text{pc}^3} \right). \quad (1.2)$$

An important property of cross sections of self-interacting dark matter particles, inferred from fits to observational data, is that they should decrease as a function of the relative velocities  $v_{\text{rel}}$  of these DM particles. Quantitatively, fits to galactic data on the scale of  $\sim 1–10$  kpc, with velocities  $v_{\text{rel}} \sim 50–200$  km/s, yield values  $\sigma/m_{\text{DM}} \sim 1 \text{ cm}^2/\text{g}$ , while fits to observations of galaxy clusters on distance scales of several Mpc and  $v_{\text{rel}} \sim O(10^3)$  km/s generally yield smaller values of  $\sigma/m_{\text{DM}} \sim 0.1 \text{ cm}^2/\text{g}$  (note the conversion relation  $1 \text{ cm}^2/\text{g} = 1.8 \text{ barn}/\text{GeV}$ ).

In this paper we consider SIDM models in which the dark matter is comprised of a spin-1/2 Dirac fermion  $\chi$ , interacting with a mediator, generically denoted  $\xi$ . Both the DM fermion and the mediator are taken to be singlets under the Standard Model (SM). We study two versions of this model, namely one in which the mediator field is a real scalar,  $\phi$ , and another in which the mediator is a vector field,  $\xi = V$ . In both versions, we work in the context of an asymmetric dark matter (ADM) theory (for a review, see, e.g., [41]). Thus, by the time at which large-scale structure formation begins, a net asymmetry has built up in the number density of  $\chi$  and  $\bar{\chi}$  particles. By convention, we take this asymmetry to be such that the number density of  $\chi$  particles is dominant over that of  $\bar{\chi}$  particles. We assume parameter values such that the lowest-order perturbative calculation of the cross section gives a reliable description of the physics, so we do not need to deal with nonperturbative effects and bound states of dark matter particles. We compute the scattering cross section  $\sigma$ , the transfer cross section  $\sigma_T$ , and the

<sup>1</sup> See, e.g., Particle Data Group, Review of Particle Properties online at <http://pdg.lbl.gov> and L. Baudis and S. Profumo, [Dark Matter Minireview](#) at this website.

<sup>2</sup> Specifically, defining  $\Omega_i \equiv \rho_i/\rho_c$ , where  $\rho_c = 3H_0^2/(8\pi G)$ , with  $H_0$  the current Hubble constant,  $G$  the Newton gravitational constant, and  $\rho_i$  the mass density of a constituent  $i$ , current cosmological observations yield the results  $\Omega_m = 0.315(7)$  for the matter density,  $\Omega_{\text{DM}} = 0.265(7)$  for the dark matter density, and  $\Omega_b = 0.0493(6)$  for the baryon matter density (see [Particle Data Group online](#)).

viscosity cross section  $\sigma_V$  for this reaction. As one part of our study, we give analytic and numerical comparisons of results obtained with the inclusion of both  $t$ -channel and  $u$ -channel exchanges and results obtained in an approximation that has often been used in the literature that includes only the  $t$ -channel contribution. Our new results provide improved accuracy for fitting models with self-interacting dark matter to observational data.

In the version of our SIDM model with a real scalar mediator  $\xi = \phi$ , we take the interaction between  $\chi$  and  $\phi$  to be of Yukawa form, as described by the interaction Lagrangian

$$\mathcal{L}_y = y_\chi [\bar{\chi}\chi]\phi. \quad (1.3)$$

In the second version, the DM fermion  $\chi$  is assumed to be charged under a  $U(1)_V$  gauge symmetry with gauge field  $V$  and gauge coupling  $g$ . Since only the product of the  $U(1)_V$  charge of  $\chi$  times  $g$  occurs in the covariant derivative in this theory, we may, without loss of generality, take this charge to be unity and denote the product as  $g_\chi$ . The corresponding interaction Lagrangian is

$$\mathcal{L}_{\chi\chi V} = g_\chi [\bar{\chi}\gamma_\mu\chi]V^\mu. \quad (1.4)$$

A Higgs-type mechanism is assumed to break the  $U(1)_V$  symmetry and give a mass  $m_V$  to the gauge field  $V$ . For compact notation, we use the same symbol,  $\alpha_\chi$ , to denote  $y_\chi^2/(4\pi)$  for the case of a scalar mediator and  $g_\chi^2/(4\pi)$  for the case of a vector mediator. For our study, it will be convenient to have one reference set of parameters, and for this purpose we will use the values

$$m_\chi = 5 \text{ GeV}, \quad m_\xi = 5 \text{ MeV}, \quad \alpha_\chi = 3 \times 10^{-4}, \quad (1.5)$$

where, as above,  $\xi$  denotes  $\phi$  or  $V$  in the two respective versions of the model. Thus, this model makes use of a light mediator. Motivations for this choice are discussed below. We will also calculate cross sections for a range of values of the coupling,  $\alpha_\chi$ , and the mediator mass,  $m_\xi$ , and show how the results compare with those obtained with the reference set of values in Eq. (1.5). Note that the  $\chi$  mass term is of Dirac form,  $\mathcal{L}_{m_\chi} = m_\chi \bar{\chi}\chi$ ; we do not consider Majorana mass terms for  $\chi$  here.

Self-interacting dark matter models of this type have been shown to ameliorate problems with excessive density on the scale of  $\sim 1$  kpc in the cores of galaxies and to improve fits to morphological properties of galaxies and, on larger length scales extending to several Mpc, also improve fits observational data on clusters of galaxies [14], [29–74]. Self-interacting dark matter models with scalar and/or vector mediators are motivated by the fact that these yield DM-DM scattering cross sections that decrease as a function of the relative velocities  $v_{\text{vel}}$  of colliding DM particles, as is desirable to fit observational data. The reason for our restriction to a vectorial gauge interaction in Eq. (1.4) is that the generalization of this to a chiral gauge theory, with an interaction  $\mathcal{L} = q_L g [\bar{\chi}_L \gamma_\mu \chi_L] V^\mu + q_R g [\bar{\chi}_R \gamma_\mu \chi_R] V^\mu$  in which the charges  $q_L \neq q_R$  would lead to triangle gauge anomalies

unless one added further DM fermions to cancel these. To maintain maximal simplicity, we have thus restricted this version of the model to the vectorial interaction (1.4).

The relative velocities of DM particles on all of the scales relevant for galactic and cluster properties are nonrelativistic. Consequently, an approach that has often been used is to model the scattering in terms of a quantum-mechanical problem with a potential of the type that would result in the nonrelativistic limit starting from the  $t$ -channel exchange of the mediator. In [62], an analysis was given of the full quantum field theoretic scattering of DM particles in the case of reaction with incident  $\chi + \bar{\chi}$ . However, Ref. [62] did not consider in depth the reaction

$$\chi + \chi \rightarrow \chi + \chi \quad (1.6)$$

that is relevant to an ADM model. In passing, we note that our analysis is equally applicable for symmetric dark matter models; however, in this case, the reaction (1.6) only contributes in part to the DM-DM scattering, the other process being  $\bar{\chi} + \chi \rightarrow \bar{\chi} + \chi$ , which was considered extensively in ref. [62]. Here we focus on the reaction (1.6).

## II. BACKGROUND

In this section we explain the reasons for our choice of parameter values (1.5) in our model. First, in asymmetric dark matter models, with the asymmetries in the dark matter and the baryons being of similar magnitude, it is plausible that

$$\frac{m_{\text{DM}}}{m_p} \simeq \frac{\rho_{\text{DM}}}{\rho_b} \simeq 5, \quad (2.1)$$

where  $\rho_b$  is the average cosmological baryon density, and  $m_p$  is the proton mass. This leads to the choice  $m_\chi \simeq 5$  GeV. (It should be noted that the simple relationship can be avoided in specific models, depending on the mechanisms that are assumed for the generation of the  $\chi$ - $\bar{\chi}$  number asymmetry [41], but it will suffice for our present purposes.) Second, as discussed above, SIDM fits to small-scale structure yield  $\sigma/m_{\text{DM}} \sim 1 \text{ cm}^2/\text{g}$ . Now, we will show that in our model,  $\sigma/m_\chi \simeq 2\pi\alpha_\chi^2 m_\chi/m_\xi^4$ . Setting this equal to  $1 \text{ cm}^2/\text{g}$  determines the mediator mass  $m_\xi$  to be

$$m_\xi = \left( \frac{\alpha_\chi}{1.2 \times 10^{-5}} \right)^{1/2} \left( \frac{m_\chi}{5 \text{ GeV}} \right)^{1/4} \text{ MeV}. \quad (2.2)$$

Third, in order to effectively annihilate away the symmetric component of the dark matter in the early universe in the ADM model, one requires a sizable cross section for  $\bar{\chi}\chi \rightarrow \xi\xi$ . Note that, from Eq. (2.2), it follows that  $m_\xi$  is naturally smaller than  $m_\chi$ , so that this process is kinematically allowed. The depletion of the symmetric component of the DM in the early Universe is satisfied

when [39, 41]

$$\langle \sigma v_{\text{rel}} \rangle_{\bar{\chi}\chi \rightarrow \xi\xi} \simeq \frac{\pi \alpha_\chi^2}{m_\chi^2} \sqrt{1 - \frac{m_\xi^2}{m_\chi^2}} \gtrsim 0.6 \times 10^{-25} \text{ cm}^3/\text{s} . \quad (2.3)$$

Anticipating that  $m_\xi \ll m_\chi$ , this then yields a lower bound on the SIDM coupling strength, namely

$$\alpha_\chi \gtrsim 2 \times 10^{-4} \left( \frac{m_\chi}{5 \text{ GeV}} \right) . \quad (2.4)$$

As stated before, for simplicity, we assume parameter values such that lowest-order perturbative calculations are sufficient to describe the scattering. From Eq. (A3) in Appendix A, this perturbativity condition requires that  $\alpha_\chi m_\chi / m_\phi \ll 1$ . Using the constraints in Eqs. (2.1), (2.2), (2.4), and (A3), we then choose the values of the parameters in eq. (1.5). Because the DM particle  $\chi$  and the mediator are SM-singlets, these choices for their masses are in accord with bounds on DM particles and mediators from current data (for summaries of bounds, see, e.g., [86–88]). Although we use the particular set of values of the parameters in Eq. (1.5) for much of our analysis, we also perform cross section calculations for a substantial range of allowed values of  $\alpha_\chi$  and  $m_\chi$  in Section VI. These calculations show how our results would change with different (allowed) values of parameters. Importantly, our choices for  $m_\chi$  and  $m_\xi$ , which are motivated from the above considerations, also lead to the desired velocity dependences for the SIDM cross sections in the model that are of the right order to fit observational data.

### III. KINEMATICS

In this section we review some basic kinematics relevant for our cross section calculations. Since the number density of  $\bar{\chi}$  fermions is much smaller than that of  $\chi$  fermions after the  $\bar{\chi}$  fermions have annihilated away in the ADM framework, the dominant self-interactions of the  $\chi$  DM particles arise from the reaction (1.6). We take  $\alpha_\chi$  to be sufficiently small that the  $\chi$ - $\xi$  interaction can be well described by lowest-order perturbation theory. This entails the condition that there be no significant Sommerfeld enhancement of the scattering. In the case of a vector mediator, the reaction (1.6) involves a repulsive interaction of the  $\chi$  particles, so there is obviously no Sommerfeld enhancement. Our choice of parameters (1.5) also guarantees the reliability of the lowest-order perturbative calculation in the scalar case, as is discussed further in Appendix A.

At tree level, there are two graphs contributing to the  $\chi + \chi \rightarrow \chi + \chi$  reaction, involving exchange of the mediator in the  $t$ -channel and  $u$ -channel, with a relative minus sign between the two terms in the amplitude, resulting from the fact that these two graphs are related by the interchange of identical fermions in the final state. These graphs and the associated momentum labelling are shown

in Fig. 1. For the reaction  $\chi(p_1) + \chi(p_2) \rightarrow \chi(p_3) + \chi(p_4)$ , we define the usual invariants

$$\begin{aligned} s &= (p_1 + p_2)^2 = (p_3 + p_4)^2 \\ t &= (p_1 - p_3)^2 = (p_4 - p_2)^2 \\ u &= (p_1 - p_4)^2 = (p_3 - p_2)^2 . \end{aligned} \quad (3.1)$$

We review some basic kinematics relevant for the analysis of this reaction. In the center-of-mass (CM) frame, the energies of each of the particles in the initial and final states are the same and are equal to

$$E_\chi = \frac{\sqrt{s}}{2} . \quad (3.2)$$

Similarly, the magnitudes of the 3-momenta of each of the particles in the initial and final states are the same and are equal to

$$|\vec{p}_\chi| = \beta_\chi \frac{\sqrt{s}}{2} , \quad (3.3)$$

where the magnitudes of the CM velocities are

$$\beta_\chi = \sqrt{1 - \frac{4m_\chi^2}{s}} . \quad (3.4)$$

In the nonrelativistic limit, the relative velocity with which the two  $\chi$  particles approach each other is

$$\beta_{\text{rel}} = 2\beta_\chi , \quad (3.5)$$

so in this limit,  $|\vec{p}_\chi| = m_\chi \beta_{\text{rel}}/2$ . The angle between  $\vec{p}_1$  and  $\vec{p}_3$  in the center of mass frame is the CM scattering angle,  $\theta$ . The invariants  $s$ ,  $t$ , and  $u$  can be written in terms of  $|\vec{p}_\chi|$  and  $\theta$  as

$$\begin{aligned} s &= 4(m_\chi^2 + |\vec{p}_\chi|^2) \\ t &= -4|\vec{p}_\chi|^2 \sin^2(\theta/2) \\ u &= -4|\vec{p}_\chi|^2 \cos^2(\theta/2) . \end{aligned} \quad (3.6)$$

The transformation  $\theta \rightarrow \pi - \theta$  interchanges the  $t$  and  $u$  channels, as is evident in (3.6), since  $\sin[(1/2)(\pi - \theta)] = \cos(\theta/2)$ .

### IV. $\chi\chi \rightarrow \chi\chi$ SCATTERING CROSS SECTIONS WITH SCALAR MEDIATOR

#### A. Differential and Total Cross Sections

The lowest-order (tree-level) amplitude for the  $\chi + \chi \rightarrow \chi + \chi$  reaction resulting from the interaction (1.3) has the form

$$\mathcal{M} = \mathcal{M}^{(t)} - \mathcal{M}^{(u)} , \quad (4.1)$$

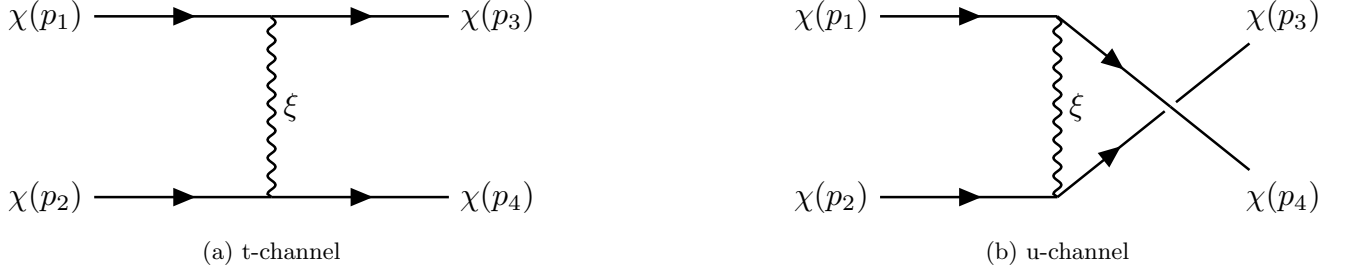


FIG. 1: Feynman diagrams for the reaction  $\chi\chi \rightarrow \chi\chi$  via the exchange of the mediator particle,  $\xi$ . We show the case where  $\xi = V$ . In standard notation, replacing the wavy line by a dashed line represents the case where  $\xi = \phi$ .

where  $\mathcal{M}^{(t)}$  and  $\mathcal{M}^{(u)}$  are the  $t$ -channel and  $u$ -channel contributions, and the relative minus sign accounts for exchanging identical fermions in the final state. The Lorentz-invariant differential cross section is

$$\frac{d\sigma}{dt} = \frac{1}{16\pi\lambda(s, m_\chi^2, m_\chi^2)} \overline{\sum} |\mathcal{M}|^2, \quad (4.2)$$

where  $\lambda(x, y, z) = x^2 + y^2 + z^2 - 2(xy + yz + zx)$ , and  $\overline{\sum}$  denotes an average over initial spins and a sum over

final spins. Here,  $\lambda(s, m_\chi^2, m_\chi^2) = (s\beta_\chi)^2$ . For our discussion, it will be useful to distinguish the terms in  $d\sigma/dt$  arising from  $\overline{\sum} |\mathcal{M}^{(t)}|^2$ ,  $\overline{\sum} |\mathcal{M}^{(u)}|^2$ , and  $\overline{\sum} [\mathcal{M}^{(t)*} \mathcal{M}^{(u)} + \mathcal{M}^{(u)*} \mathcal{M}^{(t)}] = 2\overline{\sum} \text{Re}[\mathcal{M}^{(t)*} \mathcal{M}^{(u)}]$ . We denote these as  $d\sigma^{(t)}/dt$ ,  $d\sigma^{(u)}/dt$ , and  $d\sigma^{(tu)}/dt$ , respectively. We find

$$\frac{d\sigma}{dt} = \frac{\pi\alpha_\chi^2}{(\beta_\chi s)^2} \left[ \frac{(t - 4m_\chi^2)^2}{(t - m_\phi^2)^2} + \frac{(u - 4m_\chi^2)^2}{(u - m_\phi^2)^2} - \frac{1}{(t - m_\phi^2)(u - m_\phi^2)} \left\{ \frac{1}{2}(t^2 + u^2 - s^2) + 8m_\chi^2 s - 8m_\chi^4 \right\} \right]. \quad (4.3)$$

The first and second terms on the right-hand side (RHS) of Eq. (4.2) are  $d\sigma^{(t)}/dt$  and  $d\sigma^{(u)}/dt$ , while the third term with curly brackets is  $d\sigma^{(tu)}/dt$ . Since the amplitude (4.1) is antisymmetric under interchange of identical particles in the final state, and equivalently under interchange of the  $t$ -channel and  $u$ -channel terms, it follows that the square of the amplitude is symmetric under this interchange. This symmetry under the interchange  $t \leftrightarrow u$  is evident in the RHS of Eq. (4.2). The center-of-mass cross section,  $(d\sigma/d\Omega)_{\text{CM}}$ , is related to  $d\sigma/dt$  as

$$\left( \frac{d\sigma}{d\Omega} \right)_{\text{CM}} = \frac{\lambda(s, m_\chi^2, m_\chi^2)}{4\pi s} \frac{d\sigma}{dt} = \left( \frac{\beta_\chi^2 s}{4\pi} \right) \frac{d\sigma}{dt}. \quad (4.4)$$

In terms of the center-of-mass scattering angle  $\theta$ , the symmetry of the RHS of Eq. (4.2) under the interchange  $t \leftrightarrow u$  is expressed as the symmetry

$$\left( \frac{d\sigma}{d\Omega} \right)_{\text{CM}}(\theta) = \left( \frac{d\sigma}{d\Omega} \right)_{\text{CM}}(\pi - \theta). \quad (4.5)$$

Because of the identical particles in the final state, a scattering event in which a scattered  $\chi$  particle emerges at angle  $\theta$  is indistinguishable from one in which a scattered  $\chi$  emerges at angle  $\pi - \theta$ . The total cross section for

the reaction (1.6) thus involves a symmetry factor of  $1/2$  to compensate for the double-counting involved in the integration over the range  $\theta \in [0, \pi]$ :

$$\sigma = \frac{1}{2} \int d\Omega \left( \frac{d\sigma}{d\Omega} \right)_{\text{CM}}(\pi - \theta). \quad (4.6)$$

Owing to the symmetry (4.5), this is equivalent to a polar angle integration from 0 to  $\pi/2$ :

$$\frac{1}{2} \int_{-1}^1 d\cos\theta \left( \frac{d\sigma}{d\Omega} \right)_{\text{CM}} = \int_0^1 d\cos\theta \left( \frac{d\sigma}{d\Omega} \right)_{\text{CM}}. \quad (4.7)$$

(Recall that if the final state consisted of  $n$  identical particles, the factor  $1/2$  in Eq. (4.6) would be replaced by  $1/n!$ .)

In addition to the differential cross section  $(d\sigma/d\Omega)_{\text{CM}}$ , other related (center-of-mass) differential cross sections have been used in the study of the effects of self-interacting dark matter, motivated by earlier analyses of transport properties in gases and plasmas (e.g., [89] and references therein). A major reason for this was the desire to define a differential cross section that yields a useful description of the thermalization effect of DM-DM scattering, particularly in the case where the mass of the

mediator particle is much smaller than the mass of the DM particle. In this case, to the extent that the scattering angle  $\theta$  is close to 0 for distinguishable particles or close to 0 or  $\pi$  for indistinguishable particles, the DM particle trajectories are not significantly changed by the scattering. To give greater weighting to large-angle scattering that thermalizes particles in a gas or plasma, researchers [89] have used the transfer (T) differential cross section,

$$\frac{d\sigma_T}{d\Omega} = (1 - \cos\theta) \left( \frac{d\sigma}{d\Omega} \right)_{CM} \quad (4.8)$$

and the viscosity (V) differential cross section,

$$\frac{d\sigma_V}{d\Omega} = (1 - \cos^2\theta) \left( \frac{d\sigma}{d\Omega} \right)_{CM}, \quad (4.9)$$

(Although the same symbol, V, is used for the vector mediator and viscosity, the context will always make clear which meaning is intended.) For the same reason, namely that these describe thermalization effects better than the ordinary cross section, the transfer and viscosity cross sections been used in studies of DM-DM scattering (e.g., [31, 40] and subsequent work).

Given the invariance of  $(d\sigma/d\Omega)_{CM}$  under the transformation  $\theta \rightarrow \pi - \theta$  and the fact that  $\cos\theta$  is odd under this transformation, it follows that the integral of the product of  $\cos\theta$  times  $(d\sigma/d\Omega)_{CM}$  vanishes. Hence, the total

cross section is equal to the total transfer cross section:

$$\begin{aligned} \sigma &= \frac{1}{2} \int d\Omega \left( \frac{d\sigma}{d\Omega} \right)_{CM} = \frac{2\pi}{2} \int_{-1}^1 d\cos\theta \left( \frac{d\sigma}{d\Omega} \right)_{CM} \\ &= \frac{2\pi}{2} \int_{-1}^1 d\cos\theta (1 - \cos\theta) \left( \frac{d\sigma}{d\Omega} \right)_{CM} = \sigma_T. \end{aligned} \quad (4.10)$$

As was noted in [89], the transfer differential cross section does not correctly describe the scattering in the case of identical particles, since it does not maintain the  $\theta \leftrightarrow \pi - \theta$  symmetry in the reaction. However, given Eq. (4.10), the resultant integral over angles is equal to the integral of the ordinary (unweighted) cross section, i.e.,  $\sigma_T = \sigma$ . The viscosity differential cross section, with its angle-weighting factor of  $(1 - \cos^2\theta) = \sin^2\theta$  does maintain the  $\theta \leftrightarrow \pi - \theta$  symmetry in the scattering of identical particles. In passing, we note that another type of differential cross section has also been considered that weights large-angle scattering [44], namely  $(1 - |\cos\theta|)(d\sigma/d\Omega)_{CM}$ ; this also maintains the  $\theta \rightarrow \pi - \theta$  symmetry of reaction (1.6).

In the nonrelativistic (NR) limit  $\beta_\chi \ll 1$ , the kinematic invariants have the property that  $s \gg \{|t|, |u|\}$ ;  $m_\chi^2 \gg \{|t|, |u|\}$ ; and  $s \rightarrow (2m_\chi)^2$ . Hence, in this limit, the CM differential cross section reduces to

$$\begin{aligned} \left( \frac{d\sigma}{d\Omega} \right)_{CM,NR} &= \alpha_\chi^2 m_\chi^2 \left[ \frac{1}{(t - m_\phi^2)^2} + \frac{1}{(u - m_\phi^2)^2} - \frac{1}{(t - m_\phi^2)(u - m_\phi^2)} \right] \\ &= \sigma_0 \left[ \frac{1}{(1 + r \sin^2(\theta/2))^2} + \frac{1}{(1 + r \cos^2(\theta/2))^2} - \frac{1}{(1 + r \sin^2(\theta/2))(1 + r \cos^2(\theta/2))} \right], \end{aligned} \quad (4.11)$$

where

$$\sigma_0 = \frac{\alpha_\chi^2 m_\chi^2}{m_\phi^4} \quad (4.12)$$

and  $r$  is the ratio

$$r = \left( \frac{\beta_{\text{rel}} m_\chi}{m_\phi} \right)^2. \quad (4.13)$$

The property that the transformation  $\theta \rightarrow \pi - \theta$  (under which  $\sin(\theta/2) \rightarrow \cos(\theta/2)$ ) interchanges the  $t$  and  $u$  channels is evident in Eq. (4.11), since it interchanges the first and second terms arising, respectively, from  $|\mathcal{M}^{(t)}|^2$  and from  $|\mathcal{M}^{(u)}|^2$ , and leaves the third term arising from  $-2\text{Re}(\mathcal{M}^{(t)*}\mathcal{M}^{(u)})$  invariant. Since all of the  $\chi\text{-}\chi$  relative velocities  $v_{\text{rel}}$  in the relevant observational data are

nonrelativistic, we will henceforth specialize to this case, taking the subscript NR to be implicit in the notation.

Since self-interacting dark matter has been studied extensively before, it is appropriate to discuss how our current results compare with and complement previous work. In (Eq. (25) of) the review [53] on SIDM, the differential cross section in the center of mass for elastic DM self-scattering was given (in the same perturbative Born regime  $\alpha_\chi m_\chi/m_\phi \ll 1$  as we use here) as

$$\frac{d\sigma}{d\Omega} = \frac{\alpha_\chi^2 m_\chi^2}{[m_\chi^2 v_{\text{rel}}^2 (1 - \cos\theta)/2 + m_\phi^2]^2} \equiv \frac{\sigma_0}{[r \sin^2(\theta/2) + 1]^2}, \quad (4.14)$$

where we transcribe the result from [53] in our notation in the second term of Eq. (4.14). As is evident, this corresponds to the  $t$ -channel contribution in our full result (4.11). However, the true differential cross section for the

DM self-scattering  $\chi + \chi \rightarrow \chi + \chi$  must include not just the  $t$ -channel contribution but also the  $u$ -channel contribution, as we have done here. A subsequent study in [68] focused on a regime where nonperturbative effects are important and gave results for DM-DM scattering with both identical and non-identical particles. Our work is complementary to [68], since we choose parameters in Eq. (1.5) such that nonperturbative effects are not important.

Regarding the range of values of the ratio  $r$  in Eq. (4.13), it is important to note that even in the nonrelativistic regime  $\beta_{\text{rel}} \ll 1$ , it is not necessarily the case that the ratio  $r$  is small. With the illustrative mass values in Eq. (1.5), and taking into account that for  $v_{\text{rel}} \sim 3 \times 10^3$  km/s (i.e.,  $\beta_{\text{rel}} \sim 10^{-2}$ ) for DM particles in galaxy clusters, it follows that  $r \sim 10^2$  in this case. In contrast, for the analysis of DM self-interactions on length scales of order a few kpc within a galaxy, if  $v_{\text{rel}} \sim 30$  km/sec (i.e.,  $\beta_{\text{rel}} \sim 10^{-4}$ ), then  $r \sim O(10^{-2})$ .

It is interesting to elucidate how the various contributions to the cross section from  $|\mathcal{M}^{(t)}|^2$ ,  $|\mathcal{M}^{(u)}|^2$ , and  $2\text{Re}(\mathcal{M}^{(t)*}\mathcal{M}^{(u)})$  behave as a function of  $r$ . We find that in the  $r \ll 1$  regime relevant for the analysis of galactic data on the 1-10 kpc scale, the terms contributing to  $(d\sigma/d\Omega)_{\text{CM}}$  have the property that the  $t$ -channel term  $|\mathcal{M}^{(t)}|^2$  and the  $u$ -channel term  $|\mathcal{M}^{(u)}|^2$  give equal contributions, while the  $t$ - $u$  interference term  $2\text{Re}(\mathcal{M}^{(t)*}\mathcal{M}^{(u)})$  gives a contribution equal in magnitude and opposite in sign to that from  $|\mathcal{M}^{(u)}|^2$ . As we denoted the three terms contributing to  $d\sigma/dt$ , we similarly label the three terms contributing to  $(d\sigma/d\Omega)_{\text{CM}}$  and the resultant total cross section with superscripts  $(t)$ ,  $(u)$ , and  $(tu)$ , so that the respective contribution to the total cross section are

$$\sigma^{(i)} \equiv \frac{1}{2} \int \left( \frac{d\sigma^{(i)}}{d\Omega} \right)_{\text{CM}} d\Omega, \quad i = t, u, tu, \quad (4.15)$$

and

$$\sigma = \sigma^{(t)} + \sigma^{(u)} + \sigma^{(tu)}. \quad (4.16)$$

We calculate

$$\sigma^{(t)} = \sigma^{(u)} = \frac{2\pi\sigma_0}{1+r} \quad (4.17)$$

and

$$\sigma^{(tu)} = -4\pi\sigma_0 \frac{\ln(1+r)}{r(2+r)}, \quad (4.18)$$

so that

$$\sigma = 4\pi\sigma_0 \left[ \frac{1}{1+r} - \frac{\ln(1+r)}{r(2+r)} \right]. \quad (4.19)$$

For fixed  $\sigma_0$ , the total cross section  $\sigma$  is a monotonically decreasing function of the ratio  $r$ . Concerning the individual contributions to  $\sigma$ , we observe that

$$\sigma^{(t)} = \sigma^{(u)} = -\sigma^{(tu)} = 2\pi\sigma_0 \quad \text{at } r = 0, \quad (4.20)$$

so that for small  $r$ , there is a cancellation between the interference term  $\sigma^{(tu)}$  and the  $u$ -channel term  $\sigma^{(u)}$  (or equivalently, the  $t$ -channel term, since  $\sigma^{(t)} = \sigma^{(u)}$ ). In contrast, for large  $r$ ,  $\sigma^{(t)} = \sigma^{(u)}$  decrease as  $2\pi\sigma_0/r$ , while  $\sigma^{(tu)}$  decreases more rapidly, as  $\sigma^{(tu)} \sim -4\pi\sigma_0 \ln r/r^2$ . The total cross section has the small- $r$  Taylor series expansion

$$\sigma = 2\pi\sigma_0 \left[ 1 - r + \frac{7}{6}r^2 + O(r^3) \right] \quad \text{for } r \ll 1. \quad (4.21)$$

For  $r \gg 1$ ,  $\sigma$  has the series expansion

$$\sigma = \frac{4\pi\sigma_0}{r} \left[ 1 - \frac{(1+\ln r)}{r} + O\left(\frac{\ln r}{r^2}\right) \right] \quad \text{for NR regime and } r \gg 1. \quad (4.22)$$

The prefactor in Eq. (4.22) is

$$\frac{4\pi\sigma_0}{r} = \frac{4\pi\alpha_\chi^2}{m_\phi^2\beta_{\text{rel}}^2}. \quad (4.23)$$

To compare the full cross section with the result obtained by including only the contribution from the  $t$ -channel, we consider the ratio

$$\frac{\sigma}{\sigma^{(t)}} = 2 \left[ 1 - \frac{(1+r)\ln(1+r)}{r(2+r)} \right]. \quad (4.24)$$

This ratio has the small- $r$  expansion

$$\frac{\sigma}{\sigma^{(t)}} = 1 + \frac{r^2}{6} - \frac{r^3}{6} + O(r^4) \quad \text{for } r \ll 1, \quad (4.25)$$

so in the small- $r$  regime,  $\sigma$  is approximately equal to  $\sigma^{(t)}$ . For the (nonrelativistic) large- $r$  regime, the ratio (4.24) has the expansion

$$\frac{\sigma}{\sigma^{(t)}} = 2 \left[ 1 - \frac{\ln r}{r} + \frac{\ln r - 1}{r^2} + O\left(\frac{\ln r}{r^3}\right) \right] \quad \text{for NR regime and } r \gg 1. \quad (4.26)$$

Thus, in this large- $r$  regime relevant for fits to observational data on galaxy clusters, the full  $\chi$ - $\chi$  scattering cross section is larger by approximately a factor of 2 than the result obtained by keeping only the contribution from the  $t$ -channel.

In order to compare the full calculation including contributions from both the  $t$ -channel and  $u$ -channel with a calculation that only includes the  $t$ -channel, we plot  $\sigma$  versus  $\sigma^{(t)}$  in Fig. 2 as a function of  $v_{\text{rel}}$ . For this purpose, we use the illustrative values of masses and couplings in Eq. (1.5). In accordance with our result (5.2) below, we subsume the cases of a scalar and a vector mediator together and denote  $m_\xi$  as the mass of  $\phi$  or  $V$ . We note again that with these values, there is no significant Sommerfeld enhancement of the cross section, justifying our use of the lowest-order (tree-level) perturbatively computed amplitude in the scalar case. Separately, there is no Sommerfeld enhancement in the vector

case since the scattering is repulsive. The dependence of the differential cross sections on the angle  $\theta$  is shown in the comparative Fig. 2d. As is evident from Fig. 2, for the range of relative velocities  $v_{\text{rel}} \lesssim 10^2$  km/s relevant for dark matter scattering in the interior of galaxies and dwarf spheroidal satellites,  $\sigma$  is close to  $\sigma^{(t)}$ , but as  $v_{\text{rel}}$  increases beyond about  $10^2$  km/s, although both  $\sigma$  and  $\sigma^{(t)}$  decrease, the full cross section is larger than the result obtained by keeping only the  $t$ -channel contribution. This trend continues to values  $v_{\text{rel}} \sim O(10^3)$  km/s relevant to dark matter effects in galaxy clusters. One should note that even for a fixed  $v_{\text{rel}}$ , there is considerable diversity in the values of  $\sigma/m_{DM}$  inferred from fits to galactic and cluster data (e.g., [49, 52, 71, 90] and references therein). The curves marked QM<sub>dist</sub> in Fig. 2 are the results that one would obtain in a quantum mechanical approach with a potential for the different situation with distinguishable particles (see Appendix). We show results for a specific set of  $v_{\text{rel}}$  values in Table I.

## B. Transfer Cross Sections

Our result in Eq. (4.11) together with the definition (4.8) yields the differential transfer cross section in the relevant nonrelativistic limit. For the individual contributions from  $|\mathcal{M}^{(t)}|^2$ ,  $|\mathcal{M}^{(u)}|^2$ , and  $-2\text{Re}(\mathcal{M}^{(t)*}\mathcal{M}^{(u)})$ , we calculate (in the nonrelativistic regime, as before),

$$\sigma_{\text{T}}^{(t)} = \frac{4\pi\sigma_0}{r} \left[ -\frac{1}{1+r} + \frac{\ln(1+r)}{r} \right], \quad (4.27)$$

$$\sigma_{\text{T}}^{(u)} = \frac{4\pi\sigma_0}{r} \left[ 1 - \frac{\ln(1+r)}{r} \right], \quad (4.28)$$

and

$$\sigma_{\text{T}}^{(tu)} = -\frac{4\pi\sigma_0}{r} \left[ \frac{\ln(1+r)}{2+r} \right]. \quad (4.29)$$

The prefactor in Eqs. (4.27)-(4.29) is given by Eq. (4.23). Note that, in contrast to the equality  $\sigma^{(t)} = \sigma^{(u)}$  in Eq. (4.17), the individual contributions  $\sigma_{\text{T}}^{(t)}$  and  $\sigma_{\text{T}}^{(u)}$  to  $\sigma_{\text{T}}$  are not equal; i.e.,  $\sigma_{\text{T}}^{(t)} \neq \sigma_{\text{T}}^{(u)}$ . This is a consequence of the fact that the definition of  $d\sigma_{\text{T}}/d\Omega$  fails to preserve the  $\theta \rightarrow \pi - \theta$  symmetry of the actual differential cross section for the reaction (1.6).

Summing these contributions, we find, in accordance with our general equality (4.10), the result

$$\sigma_{\text{T}} = \sigma = 4\pi\sigma_0 \left[ \frac{1}{1+r} - \frac{\ln(1+r)}{r(2+r)} \right]. \quad (4.30)$$

Since  $\sigma_{\text{T}} = \sigma$ , the transfer cross section has the same small- $r$  and large- $r$  expansions as were displayed for  $\sigma$  in Eqs. (4.21) and (4.22).

We may compare our result (4.30) for  $\sigma_{\text{T}}$  with the result given, in the same Born regime, as Eq. (A1) in Ref. [39] (denoted TYZ), which is the same as Eq. (5) in Ref. [34] (denoted FKY) and reads (with their  $R \equiv \sqrt{r}$  and  $v = \beta_{\text{rel}}$  in our notation)

$$\begin{aligned} \sigma_{\text{T};FKY,TYZ} &= \frac{8\pi\alpha_{\chi}^2}{m_{\chi}^2\beta_{\text{rel}}^4} \left[ \ln(1+r) - \frac{r}{(1+r)} \right] \\ &= \frac{8\pi\alpha_{\chi}^2 r}{m_{\chi}^2\beta_{\text{rel}}^4} \left[ \frac{\ln(1+r)}{r} - \frac{1}{1+r} \right] \\ &= \frac{8\pi\alpha_{\chi}^2}{m_{\phi}^2\beta_{\text{rel}}^2} \left[ \frac{\ln(1+r)}{r} - \frac{1}{1+r} \right]. \end{aligned} \quad (4.31)$$

As is evident from a comparison of Eq. (4.31) with our Eq. (4.27) (using the definition of our notation given in Eq. (4.23)), the result for the transfer cross section in Eq. (A1) of Ref. [39] (or equivalently, Eq. (5) of Ref. [34]) is what one would get for the DM self-scattering if one did the calculation for non-identical particles and hence only included the  $t$ -channel contribution and did not include the 1/2 factor for identical particles in the final state in performing the integral over  $d\Omega$ . That is,

$$\sigma_{\text{T},TYZ,FKY} = 2\sigma_{\text{T}}^{(t)}. \quad (4.32)$$

To compare the full transfer cross section with the result obtained by just including the  $t$ -channel contribution, we examine the ratio

$$\frac{\sigma_{\text{T}}}{\sigma_{\text{T}}^{(t)}} = \frac{r \left[ \frac{1}{1+r} - \frac{\ln(1+r)}{r(2+r)} \right]}{\left[ -\frac{1}{1+r} + \frac{\ln(1+r)}{r} \right]}. \quad (4.33)$$

For small  $r$ , this ratio has the expansion

$$\frac{\sigma_{\text{T}}}{\sigma_{\text{T}}^{(t)}} = 1 + \frac{r}{3} + \frac{r^2}{9} + O(r^3) \quad \text{for } r \ll 1. \quad (4.34)$$

For large  $r$ , we find

$$\frac{\sigma_{\text{T}}}{\sigma_{\text{T}}^{(t)}} \sim \frac{r}{\ln r - 1} \quad \text{for } r \gg 1. \quad (4.35)$$

Thus, although both our  $\sigma_{\text{T}}$  and the result  $\sigma_{\text{T},FKY,TYZ}$  decrease with  $v_{\text{rel}}$  (and thus with  $r$ , for fixed  $m_{\chi}$  and  $m_{\xi}$ ), our result decreases substantially less rapidly for large  $r$ . With our parameters, this large- $r$  regime includes values of  $v_{\text{rel}} \sim O(10^3)$  km/s typical of galaxy clusters. For example, at  $v_{\text{rel}} = 3 \times 10^3$  km/s (corresponding to  $r = 10^2$  with our choices for  $m_{\chi}$  and  $m_{\xi}$  in Eq. (1.5)), the ratio (4.33) has the value 26, or equivalently,  $\sigma_{\text{T}}/\sigma_{\text{T},FKY,TYZ} = 13$ , a substantial difference from unity. Therefore, in performing fits to observational data, if one uses the transfer cross section, we would advocate the use of Eq. (4.30) rather than the result in Eq. (A1) of Ref. [39] for the large- $r$  regime, since they differ substantially.

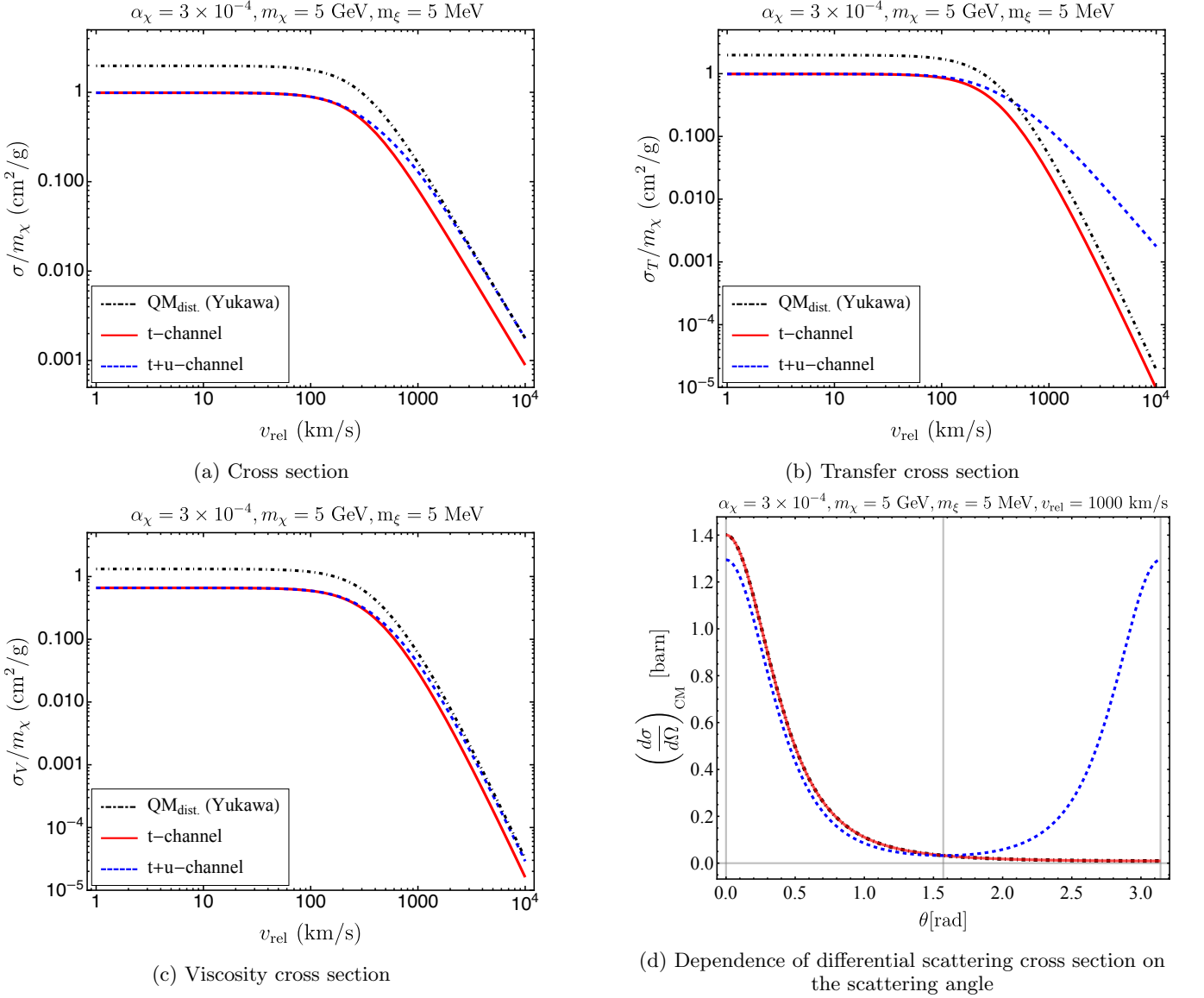


FIG. 2: Fig. 2a shows  $\sigma/m_\chi$  for the reaction  $\chi + \chi \rightarrow \chi + \chi$ , as a function of the relative velocity  $v_{\text{rel}}$  of the colliding  $\chi$  particles. The full result with proper inclusion of both  $t$ -channel and  $u$ -channel contributions is shown as the dashed curve (colored blue online), while the result of including only the  $t$ -channel, is indicated by the solid curve (colored red online). The curves marked  $\text{QM}_{\text{dist}}$  refer to the result that one would get in a quantum mechanical approach to the different situation with distinguishable particles (see Appendix). The illustrative values  $m_\chi = 5$  GeV,  $m_\xi = 5$  MeV, and  $\alpha_\chi = 3 \times 10^{-4}$  given in Eq. (1.5) are used for the calculation. Fig. 2b and Fig. 2c present the corresponding plots of the transfer and viscosity cross sections respectively. Fig. 2d shows the dependence of the differential CM scattering cross section on the scattering angle. The color coding in Fig. 2d is the same as in the other figures.

In Fig. 2b we plot  $\sigma_T$  in comparison with  $\sigma_T^{(t)}$  over the same range of  $v_{\text{rel}}$  and thus also  $\beta_{\text{rel}}$  as for the regular CM cross section. The fact that the true  $\sigma_T$  decreases considerably less rapidly than the  $t$ -channel contribution used in [34, 39] is evident in this figure. This is also apparent in Table I.

### C. Viscosity Cross Section

For the viscosity cross section we calculate the following contributions from the  $t$ -channel,  $u$ -channel, and  $t$ - $u$  interference:

$$\begin{aligned} \sigma_V^{(t)} &= \sigma_V^{(u)} \\ &= \frac{8\pi\sigma_0}{r^2} \left[ -2 + (2+r) \frac{\ln(1+r)}{r} \right] \end{aligned} \quad (4.36)$$



$v_{\text{rel}}$ (km/s)	$\sigma^{(t)}/m_\chi$ (cm <sup>2</sup> /g)	$\sigma/m_\chi$	$\sigma_T^{(t)}/m_\chi$	$\sigma_T/m_\chi$	$\sigma_V^{(t)}/m_\chi$	$\sigma_V/m_\chi$
10	0.99	0.99	0.99	0.99	0.66	0.66
10 <sup>2</sup>	0.90	0.90	0.86	0.89	0.59	0.59
10 <sup>3</sup>	0.082	0.13	0.025	0.13	0.030	0.042
10 <sup>4</sup>	$0.89 \times 10^{-3}$	$1.8 \times 10^{-3}$	$0.96 \times 10^{-5}$	$1.8 \times 10^{-3}$	$1.6 \times 10^{-5}$	$2.9 \times 10^{-5}$

TABLE I: Comparison of different cross sections divided by dark matter particle mass,  $m_\chi$ , in units of cm<sup>2</sup>/g, as functions of  $v_{\text{rel}}$ . The calculations use the parameter values in Eq. (1.5). See text for further details.

and

$$\sigma_V^{(tu)} = \frac{8\pi\sigma_0}{r^2} \left[ -1 + \frac{2(1+r)\ln(1+r)}{(2+r)r} \right], \quad (4.37)$$

so that the total nonrelativistic viscosity cross section is

$$\begin{aligned} \sigma_V &= \sigma_V^{(t)} + \sigma_V^{(u)} + \sigma_V^{(tu)} \\ &= \frac{8\pi\sigma_0}{r^2} \left[ -5 + \frac{2(5+5r+r^2)\ln(1+r)}{(2+r)r} \right]. \end{aligned} \quad (4.38)$$

As was the case with  $\sigma$  and  $\sigma_T$ , for fixed  $m_\chi$  and  $m_\phi$ , the viscosity cross section  $\sigma_V$  is a monotonically decreasing function of  $r$ .

We remark on properties of the individual contributions  $\sigma_V^{(t)}$ ,  $\sigma_V^{(u)}$ , and  $\sigma_V^{(tu)}$ . The fact that  $\sigma_V^{(t)} = \sigma_V^{(u)}$  is guaranteed by the property that  $(d\sigma/d\Omega)_V$  maintains the  $\theta \rightarrow \pi - \theta$  symmetry of  $(d\sigma/d\Omega)_{\text{CM}}$ , which interchanges the  $t$ - and  $u$ -channels. These contributions have the small- $r$  expansions

$$\begin{aligned} \sigma_V^{(t)} &= \sigma_V^{(u)} = \frac{4\pi\sigma_0}{3} \left[ 1 - r + \frac{9}{10}r^2 + O(r^3) \right] \\ &\text{for } r \ll 1 \end{aligned} \quad (4.39)$$

and

$$\begin{aligned} \sigma_V^{(tu)} &= \sigma_V^{(u)} = \frac{4\pi\sigma_0}{3} \left[ -1 + r - \frac{4}{5}r^2 + O(r^3) \right] \\ &\text{for } r \ll 1. \end{aligned} \quad (4.40)$$

Hence,

$$\begin{aligned} \lim_{r \rightarrow 0} \sigma_V^{(t)} &= \lim_{r \rightarrow 0} \sigma_V^{(u)} = - \lim_{r \rightarrow 0} \sigma_V^{(tu)} \\ &= \frac{4\pi\sigma_0}{3}. \end{aligned} \quad (4.41)$$

This is analogous to the relation that we found for the individual contributions to  $\sigma$  in Eq. (4.20). Thus, the full

viscosity cross section has the small- $r$  series expansion

$$\sigma_V = \frac{4\pi\sigma_0}{3} \left[ 1 - r + r^2 + O(r^3) \right] \quad \text{for } r \ll 1. \quad (4.42)$$

At large  $r$ ,  $\sigma_V$  has the series expansion

$$\begin{aligned} \sigma_V &= \frac{8\pi\sigma_0}{r^2} \left[ 2\ln r - 5 + \frac{2(3\ln r + 1)}{r} + O\left(\frac{\ln r}{r^2}\right) \right] \\ &\text{for } r \gg 1. \end{aligned} \quad (4.43)$$

The prefactor in Eq. (4.43) is  $8\pi\sigma_0/r^2 = 8\pi\alpha_\chi^2/(\beta_{\text{rel}}^4 m_\chi^2)$ .

For small  $r$ , the ratio  $\sigma_V/\sigma_V^{(t)}$  behaves as

$$\frac{\sigma_V}{\sigma_V^{(t)}} = 1 + \frac{r^2}{10} + O(r^3), \quad (4.44)$$

while for  $r \gg 1$ ,

$$\frac{\sigma_V}{\sigma_V^{(t)}} = 2 - \frac{1}{\ln r} + O\left(\frac{1}{(\ln r)^2}\right). \quad (4.45)$$

In Fig. 2c we plot  $\sigma_V$  in comparison with  $\sigma_V^{(t)}$  over the same range of  $\beta_{\text{rel}}$  as for the regular CM cross section. A notable feature of these numerical calculations, which is in agreement with our analytic results, is that for values of  $v_{\text{rel}} \sim O(10^3)$  km/sec typical of galaxy clusters,  $\sigma_V$  is considerably smaller than  $\sigma_T$ . This is also evident in Table I.

## V. $\chi\chi \rightarrow \chi\chi$ SCATTERING CROSS SECTIONS WITH VECTOR MEDIATOR

In this section we consider the case of a vector mediator with the SIDM interaction (1.4). The differential cross section in this case is just the analogue of the Möller cross section with the photon replaced by the massive vector boson  $V$ :

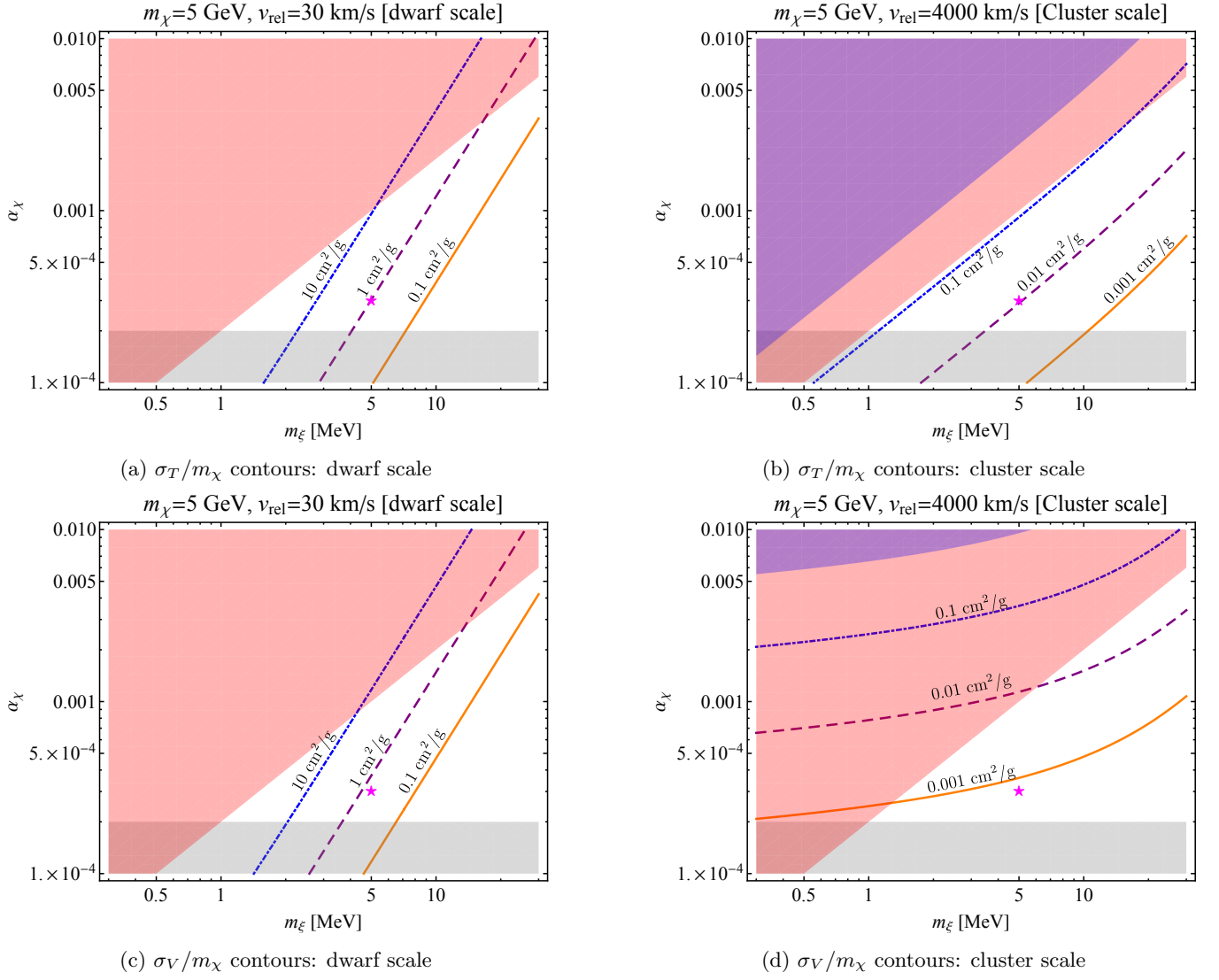


FIG. 3: Plots showing contours of fixed transfer cross section  $\sigma_T = \sigma$  and viscosity cross section  $\sigma_V$ , divided by DM mass  $m_\chi$ , in the space of parameters  $(m_\chi, \alpha_\chi)$ . Our results are calculated with the inclusion of both  $t$ -channel and  $u$ -channel contributions. The left two figures in each horizontal row apply for the typical DM-DM relative velocity  $v_{\text{rel}} = 30$  km/s in dwarfs, while the right two figures apply for the typical velocity  $v_{\text{rel}} = 4 \times 10^3$  km/s in galaxy clusters. The coupling  $\alpha_\chi$  should lie above the gray shaded region to satisfy the condition  $\langle \sigma v \rangle_{\bar{\chi}\chi \rightarrow \xi\xi} \gtrsim 0.6 \times 10^{-25} \text{ cm}^3/\text{s}$  in order to effectively deplete away the symmetric component of the DM in the early Universe. The red shaded region is outside the Born regime, namely where  $\alpha_\chi m_\chi/m_\xi > 1$ , and the blue shaded region corresponds to the exclusion limit from the Bullet cluster (Galaxy Cluster 1E 0657–56). The dot-dashed blue contour corresponds to  $\sigma_T/m_\chi = 10 \text{ cm}^2/\text{g}$ , whereas the dashed purple and solid orange contours correspond to  $\sigma_T/m_\chi = 1 \text{ cm}^2/\text{g}$  and  $0.1 \text{ cm}^2/\text{g}$ , respectively, and similarly with  $\sigma_V/m_\chi$ . In each plot, our parameter choice in Eq. (1.5) is indicated by the magenta asterisk.

$$\left( \frac{d\sigma}{d\Omega} \right)_{\text{CM}} = \frac{\alpha_\chi^2}{2s} \left[ \frac{s^2 + u^2 - 4m_\chi^2(s + u - t) + 8m_\chi^4}{(t - m_V^2)^2} + \frac{s^2 + t^2 - 4m_\chi^2(s + t - u) + 8m_\chi^4}{(u - m_V^2)^2} \right] + \frac{2\{s^2 - 8m_\chi^2 s + 12m_\chi^4\}}{(t - m_V^2)(u - m_V^2)} \quad (5.1)$$

In the nonrelativistic limit that is relevant for fitting observational data, this differential cross section becomes

the same as the result for an SIDM model with a scalar

mediator, Eq. (4.11), with the replacement  $m_\phi \rightarrow m_V$ :

$$\left(\frac{d\sigma}{d\Omega}\right)_{\text{CM,vec}} = \left(\frac{d\sigma}{d\Omega}\right)_{\text{CM},\phi} \quad \text{with } m_\phi \leftrightarrow m_V \text{ for } \beta_{\text{rel}} \ll 1, \quad (5.2)$$

where we append subscripts to indicate vector (vec) versus scalar mediators. Quantitatively, the difference between  $(d\sigma/d\Omega)_{\text{CM,vec}}$  and  $(d\sigma/d\Omega)_{\text{CM},\phi}$  is a term of  $O(\beta_{\text{rel}}^2)$ . Even at the length scale of a few Mpc in galaxy clusters,  $\beta_{\text{rel}} \sim 10^{-2}$ , and therefore this difference is negligibly small. Consequently, our analysis in the previous section also applies to this model. Similar comments apply for the transfer and viscosity cross sections.

## VI. STUDY OF PARAMETER VARIATION

In this section we study the dependence of the cross sections divided by DM mass for reaction (1.6) (calculated with both the  $t$ -channel and  $u$ -channel contributions) on the values of the coupling,  $\alpha_\chi$ , and mediator mass,  $m_\xi$ . In Fig. 3 we show plots of  $\sigma/m_\chi = \sigma_T/m_\chi$ , and  $\sigma_V/m_\chi$  as functions of  $\alpha_\chi$  and  $m_\xi$ . For this study, it will suffice to keep  $m_\chi$  fixed at the value of 5 GeV as in Eq. (1.5). The figures in the upper and lower panel are for  $\sigma/m_\chi = \sigma_T/m_\chi$ , and  $\sigma_V/m_\chi$ , respectively. In each horizontal panel, the figures on the left and right are for the value  $v_{\text{rel}} = 30$  km/s typical of dwarf satellite galaxies and the value  $4 \times 10^3$  km/s typical of galaxy clusters, respectively. In each figure we show curves of the respective cross section divided by  $m_\chi$  for the values  $10 \text{ cm}^2/\text{g}$ , (dot-dashed blue),  $1 \text{ cm}^2/\text{g}$ , (dashed purple), and  $0.1 \text{ cm}^2/\text{g}$ , (solid orange). The coupling  $\alpha_\chi$  should lie above the grey region in order to satisfy the bound  $\langle\sigma v\rangle_{\bar{\chi}\chi \rightarrow \xi\xi} \gtrsim 0.6 \times 10^{-25} \text{ cm}^3/\text{s}$  from the depletion of the symmetric component constraint on this ADM model, as discussed in Section II. The region shaded red is outside the Born regime and corresponds to  $\alpha_\chi m_\chi/m_\xi > 1$ . The region shaded blue is excluded by observational data on the Bullet Cluster (Galaxy Cluster 1E 0657-56) [32, 53]. Our parameter values in Eq. (1.5) are indicated by the magenta-colored asterisk. These plots show how  $m_\chi$  and  $m_\xi$  can be varied while retaining cross section values that avoid excluded regions. For a given choice of parameter values, our calculations (with inclusion of both  $t$ -channel and  $u$ -channel contributions) yield  $\sigma_V \ll \sigma_T$  at  $v_{\text{rel}}$  values characteristic of galaxy clusters. In both cases, our resulting cross sections are in accord with upper limits on  $\sigma/m_{\text{DM}}$  inferred from fits to properties of galaxy clusters.

## VII. CONCLUSIONS

In summary, in this paper we have studied a model with self-interacting dark matter consisting of a Dirac fermion  $\chi$  coupled to a scalar or vector mediator such that the reaction  $\chi + \chi \rightarrow \chi + \chi$  is well described by

perturbation theory. An asymmetric dark matter framework is assumed for this study. We have computed the scattering cross section for this reaction including both  $t$ -channel and  $u$ -channel contributions and have analyzed how the results with inclusion of contributions from both of these channels compare with a calculation that has often been used in the literature that only includes the  $t$ -channel contribution. Our results elucidate the interplay between the terms  $|\mathcal{M}^{(t)}|^2$ ,  $|\mathcal{M}^{(u)}|^2$ , and the interference term  $-2\text{Re}(\mathcal{M}^{(t)*}\mathcal{M}^{(u)})$  in both the differential and total cross sections. We find a particularly strong deviation at large  $r$  from results in the literature for the transfer cross section  $\sigma_T$  that include only  $t$ -channel contributions. With the illustrative values of the dark matter fermion mass  $m_\chi$ , the mediator mass  $m_\xi$ , and the coupling  $\alpha_\chi$  used here, the region of large  $r$  corresponds to DM velocities  $v_{\text{rel}} \sim 10^3$  km/s, which occur in galaxy clusters. Further, we have studied how our cross section calculations vary for a range of mediator mass  $m_\xi$  and DM-mediator coupling  $\alpha_\chi$ . Our analytic and numerical calculations should be useful in fits to observational data. A self-interacting dark matter model of the type considered here remains an appealing approach to accounting for this data on scales ranging from 1-10 kpc in galaxies to several Mpc in galaxy clusters.

## Acknowledgments

One of us (R.S.) thanks Prof. S. Nussinov for useful discussions. This research was supported in part by the U.S. National Science Foundation Grant NSF-PHY-1915093 (R.S.).

## Appendix A: Condition for the validity of the Born approximation

In this appendix we discuss further some aspects of the  $\chi + \chi \rightarrow \chi + \chi$  reaction. We comment first on the relation between our full quantum field theoretic calculation and the nonrelativistic quantum mechanical analysis in the nonrelativistic limit, where one considers scattering of the  $\chi$  particle in a potential. This relation is relevant since the velocities that occur, both on length scales of galaxies ( $v_{\text{rel}} \sim 30 - 200$  km/s), and on length scales relevant for galaxy clusters ( $v_{\text{rel}} \sim O(10^3)$  km/s), are all nonrelativistic. A standard reduction of a two-body problem of the scattering of two different particles  $a$  and  $b$  expresses this in terms of an effective one-body problem in which a particle with the reduced mass  $\mu = m_a m_b / (m_a + m_b)$  undergoes a scattering due to an isotropic potential  $V$ . For the equal-mass situation under consideration here, the particle has  $\mu = m_\chi/2$  and velocity  $v_{\text{rel}} = 2v_\chi$ , and hence momentum  $p = \mu v_{\text{rel}} = (m_\chi/2)(2v_\chi) = m_\chi v_\chi = |\vec{p}_\chi|$ , where  $|\vec{p}_\chi|$  was given in Eq. (3.3). The corresponding magnitude of the wavevector is  $k = p/\hbar \equiv p$  in our units with  $\hbar = 1$ .

A common approach is to use the Born approximation to describe a sufficiently weak scattering process. The condition for the Born approximation to be valid in the quantum mechanical analysis of potential scattering takes two different forms depending on  $|\vec{p}|$ . In both cases, it is essentially the condition that the scattered wave is a small perturbation on the incident plane wave. We use the fact that in this quantum mechanical approach, the interaction mediated by  $\xi$  exchange is represented by a potential,

$$V(\vec{x}) = V(|\vec{x}|) = V_0 \frac{e^{-m_\xi |\vec{x}|}}{m_\xi |\vec{x}|} \quad (\text{A1})$$

with

$$\frac{V_0}{m_\xi} = \alpha_\chi . \quad (\text{A2})$$

We define the distance  $|\vec{x}| \equiv d$ . The range of this potential is  $\sim a = 1/m_\xi$ . The condition for the validity of the Born approximation takes the following two forms [91], depending on the value of  $ka = p/m_\xi = \beta_\chi m_\chi/m_\xi = \sqrt{r}/2$ , where  $r$  is the ratio (4.13). For  $r \ll 1$ , the condition is that the kinetic energy  $1/(2\mu a^2)$  should be much larger than the potential energy  $\sim V_0$ , i.e.,  $2\mu a^2 V_0 \ll 1$ . Substituting  $a = 1/m_\xi$  and the expression for  $V_0$  in Eq. (A2), this is the inequality

$$\frac{2\mu V_0}{m_\xi^2} = \frac{\alpha_\chi m_\chi}{m_\xi} \ll 1 . \quad (\text{A3})$$

For  $r \gg 1$ , the condition is  $(V_0 a/\beta_{\text{rel}}) \ln(2ka) \ll 1$ , which can be rewritten as

$$\frac{\alpha_\chi}{\beta_{\text{rel}}} \ln(\sqrt{r}) \ll 1 . \quad (\text{A4})$$

To show that our parameter choices in Eq. (1.5) satisfy these conditions, we first consider values of  $v_{\text{rel}} \sim 30$  km/s relevant for SIDM dynamics within galaxies. Then  $\beta_{\text{rel}} = 10^{-4}$  so  $r = (\beta_{\text{rel}} m_\chi/m_\xi)^2 = 10^{-2}$ . Since this is  $\ll 1$ , condition (A3) is applicable. We have  $\alpha_\chi m_\chi/m_\xi = 0.3$  for our choices of parameters in Eq. (1.5). For a value of  $v_{\text{rel}} \sim 3 \times 10^3$  km/s relevant for galaxy clusters,  $\beta_{\text{rel}} = 10^{-2}$ , so  $r = 10^2$ , and hence condition (A4) applies. For this value of  $v_{\text{rel}}$ , the left-hand side of the inequality (A4) is 0.069, which is  $\ll 1$ . Thus, as stated in the text, with our choices of  $\alpha_\chi$ ,  $m_\chi$ , and  $m_\xi$  and for the values of  $v_{\text{rel}}$  of relevance to SIDM effects on scales ranging from 1-10 kpc in the core of a galaxy to several Mpc for clusters of galaxies, our restriction to the Born regime is justified.

## Appendix B: Quantum Mechanical Treatment of the Yukawa Potential

Here we review the quantum mechanical treatment of the Yukawa potential and derive Eq. (4.27) for the transfer cross section from the partial wave analysis. These are

well-known results (e.g., [91, 92]), but we briefly discuss them here for the convenience of the reader in comparing the quantum mechanical treatment with the quantum field theory results. In a quantum mechanical analysis, one writes the full wave function as consisting of an incident term (choosing the initial direction of propagation to be along the  $z$  axis, with no loss of generality) plus the spherical wave due to the scattering by the potential. For large distance  $d$  from the origin, this has the form

$$\psi(\vec{x}) = e^{ikz} + f(\theta) \frac{e^{ikd}}{d} , \quad (\text{B1})$$

where  $k = |\vec{k}|$  is the magnitude of the wave vector of the incident particle and we have assumed azimuthal symmetry. The scattering amplitude  $f(\theta)$  can be expanded in terms of partial waves as

$$f(\theta) = \frac{1}{k} \sum_{\ell=0}^{\infty} (2\ell+1) A_\ell P_\ell(\cos \theta) , \quad (\text{B2})$$

where  $P_\ell(\cos \theta)$  is the Legendre polynomial and

$$A_\ell = e^{i\delta_\ell} \sin \delta_\ell \quad (\text{B3})$$

is the quantum mechanical scattering amplitude in the  $\ell$ 'th partial wave, with phase shift  $\delta_\ell$ . The differential scattering cross section is then

$$\begin{aligned} \frac{d\sigma}{d\Omega} &= |f(\theta)|^2 \\ &= \frac{1}{k^2} \sum_{\ell, \ell'=0}^{\infty} (2\ell+1)(2\ell'+1) A_\ell A_{\ell'}^* P_\ell(\cos \theta) P_{\ell'}(\cos \theta) . \end{aligned} \quad (\text{B4})$$

Given a potential  $V(\vec{x}')$ , the Born approximation to  $f$  is

$$f = -\frac{\mu}{2\pi} \int d^3 \vec{x}' e^{-i\vec{k}' \cdot \vec{x}'} V(\vec{x}') e^{i\vec{k} \cdot \vec{x}'} \quad (\text{B5})$$

where  $\vec{k}$  and  $\vec{k}'$  are the wave vectors of the incident and scattered waves. This is evidently the Fourier transform of  $V(\vec{x}')$  with respect to the momentum transfer  $\vec{q} = \vec{k} - \vec{k}'$ , with magnitude

$$q \equiv |\vec{q}| = 2k \sin(\theta/2) . \quad (\text{B6})$$

Consider the Yukawa potential (with  $d = |\vec{x}|$ ):

$$V(d) = \pm \alpha_\chi \frac{e^{-m_\xi d}}{d} . \quad (\text{B7})$$

A standard calculation yields the scattering amplitude

$$f_{\text{Yuk}}(\theta) = \mp \frac{2\mu \alpha_\chi}{m_\xi^2 + q^2} . \quad (\text{B8})$$

For our application to  $\chi$ - $\chi$  scattering, the reduced mass is  $\mu = m_\chi/2$  and  $k = (m_\chi/2)v_{\text{rel}}$ , i.e.,  $q = m_\chi v_{\text{rel}} \sin(\theta/2)$ . Therefore, from Eq. (B4), in the Born approximation,

$$\begin{aligned} \left( \frac{d\sigma}{d\Omega} \right)_{\text{Yuk}} &= \frac{\alpha_\chi^2 m_\chi^2}{(m_\xi^2 + m_\chi^2 v_{\text{rel}}^2 \sin^2(\theta/2))^2} \\ &= \frac{\sigma_0}{(1 + r \sin^2(\theta/2))^2}, \end{aligned} \quad (\text{B9})$$

where we have used the definitions of  $\sigma_0$  and  $r$  in Eqs. (4.12) and (4.13). Comparing Eq. (B9) with Eq. (4.11), one sees that if one were to approach the calculation without proper use of the antisymmetrization of the quantum mechanical wave function, then the Yukawa potential would correspond to inclusion of only the  $t$ -channel contribution to the full quantum field theoretic amplitude. Finally, applying the definitions of transfer and viscosity cross sections, given in Eqs. (4.8, 4.9) yields the corresponding cross sections for this Yukawa potential:

$$\sigma_{\text{CM,Yuk}} = \frac{4\pi\sigma_0}{1+r}, \quad (\text{B10})$$

$$\sigma_{\text{T,Yuk}} = \frac{8\pi\sigma_0}{r} \left[ -\frac{1}{1+r} + \frac{\ln(1+r)}{r} \right], \quad (\text{B11})$$

$$\sigma_{\text{V,Yuk}} = \frac{16\pi\sigma_0}{r^2} \left[ -2 + (2+r) \frac{\ln(1+r)}{r} \right]. \quad (\text{B12})$$

Thus, these are the cross sections that one would get in a quantum mechanical treatment if one did not take account of the necessity of antisymmetrizing the wave function under exchange of identical fermions.

The calculation in nonrelativistic quantum mechanics for identical fermion scattering must, of course, respect the Pauli exclusion principle. In other words, the wavefunction for the  $\chi - \chi$  system should be completely antisymmetric, i.e., should have the form of a Slater determinant, namely

$$\Psi(x_1, x_2) = \frac{1}{\sqrt{2}} \begin{vmatrix} \chi_1(x_1) & \chi_2(x_1) \\ \chi_1(x_2) & \chi_2(x_2) \end{vmatrix}. \quad (\text{B13})$$

From here, it is evident that the normalization factor  $1/\sqrt{2}$  in the Slater determinant wavefunction is equivalent to the factor  $1/2$  in the formula for the scattering cross section (4.6). The antisymmetrization in the Slater determinant is the quantum mechanical equivalent of the inclusion of both the  $t$ -channel and the  $u$ -channel diagrams in the quantum field theoretic calculation. Thus, a quantum mechanical treatment with proper antisymmetrization for scattering of identical fermions gives the same result as the (nonrelativistic limit of the) quantum field theoretic calculation. We have presented the results for these cross sections for the Born regime in the text, as Eqs. (4.19), (4.30), and (4.38).

- 
- [1] G. R. Blumenthal, S. M. Faber, J. R. Primack, and M. J. Rees, *Nature* **311**, 517 (1984).
  - [2] M. Srednicki, R. Watkins, and K. A. Olive, *Nucl. Phys. B* **310**, 693 (1988).
  - [3] J. F. Navarro, C. S. Frenk, and S. D. M. White, *Astrophys. J.* **462**, 563 (1996), [arXiv:astro-ph/9508025](#).
  - [4] J. F. Navarro, C. S. Frenk, and S. D. M. White, *Astrophys. J.* **490**, 493 (1997), [arXiv:astro-ph/9611107](#).
  - [5] A. V. Kravtsov, A. A. Klypin, J. S. Bullock, and J. R. Primack, *Astrophys. J.* **502**, 48 (1998), [arXiv:astro-ph/9708176](#).
  - [6] B. Moore, S. Ghigna, F. Governato, G. Lake, T. R. Quinn, J. Stadel, and P. Tozzi, *Astrophys. J. Lett.* **524**, L19 (1999), [arXiv:astro-ph/9907411](#).
  - [7] J. Wang, S. Bose, C. S. Frenk, L. Gao, A. Jenkins, V. Springel, and S. D. M. White, *Nature* **585**, 39 (2020), [arXiv:1911.09720 \[astro-ph.CO\]](#).
  - [8] G. Jungman, M. Kamionkowski, and K. Griest, *Phys. Rept.* **267**, 195 (1996), [arXiv:hep-ph/9506380](#).
  - [9] J. Binney and S. Tremaine, *Galactic Dynamics: Second Edition* (2008).
  - [10] G. Bertone, D. Hooper, and J. Silk, *Phys. Rept.* **405**, 279 (2005), [arXiv:hep-ph/0404175](#).
  - [11] L. E. Strigari, *Phys. Rept.* **531**, 1 (2013), [arXiv:1211.7090 \[astro-ph.CO\]](#).
  - [12] M. Lisanti, in *Theoretical Advanced Study Institute in Elementary Particle Physics: New Frontiers in Fields and Strings* (2017) pp. 399–446, [arXiv:1603.03797 \[hep-ph\]](#).
  - [13] G. Bertone and D. Hooper, *Rev. Mod. Phys.* **90**, 045002 (2018), [arXiv:1605.04909 \[astro-ph.CO\]](#).
  - [14] D. N. Spergel and P. J. Steinhardt, *Phys. Rev. Lett.* **84**, 3760 (2000), [arXiv:astro-ph/9909386](#).
  - [15] M. Boylan-Kolchin, J. S. Bullock, and M. Kaplinghat, *Mon. Not. Roy. Astron. Soc.* **422**, 1203 (2012), [arXiv:1111.2048 \[astro-ph.CO\]](#).
  - [16] M. Boylan-Kolchin, J. S. Bullock, and M. Kaplinghat, *Mon. Not. Roy. Astron. Soc.* **415**, L40 (2011), [arXiv:1103.0007 \[astro-ph.CO\]](#).
  - [17] V. Springel, *Mon. Not. Roy. Astron. Soc.* **364**, 1105 (2005), [arXiv:astro-ph/0505010](#).
  - [18] V. Springel *et al.*, *Nature* **435**, 629 (2005), [arXiv:astro-ph/0504097](#).
  - [19] C. Scannapieco *et al.*, *Mon. Not. Roy. Astron. Soc.* **423**, 1726 (2012), [arXiv:1112.0315 \[astro-ph.GA\]](#).
  - [20] T. K. Chan, D. Kereš, J. Oñorbe, P. F. Hopkins, A. L. Muratov, C. A. Faucher-Giguère, and E. Quataert, *Mon. Not. Roy. Astron. Soc.* **454**, 2981 (2015), [arXiv:1507.02282 \[astro-ph.GA\]](#).
  - [21] A. R. Wetzel, P. F. Hopkins, J.-h. Kim, C.-A. Faucher-Giguère, D. Keres, and E. Quataert, *Astrophys. J. Lett.* **827**, L23 (2016), [arXiv:1602.05957 \[astro-ph.GA\]](#).
  - [22] T. Sawala *et al.*, *Mon. Not. Roy. Astron. Soc.* **457**, 1931 (2016), [arXiv:1511.01098 \[astro-ph.GA\]](#).
  - [23] J. S. Bullock and M. Boylan-Kolchin, *Ann. Rev. As-*

- tron. Astrophys. **55**, 343 (2017), arXiv:1707.04256 [astro-ph.CO] .
- [24] S. Y. Kim, A. H. G. Peter, and J. R. Hargis, *Phys. Rev. Lett.* **121**, 211302 (2018), arXiv:1711.06267 [astro-ph.CO] .
- [25] A. Fitts *et al.*, *Mon. Not. Roy. Astron. Soc.* **490**, 962 (2019), arXiv:1811.11791 [astro-ph.GA] .
- [26] K. E. Chua, A. Pillepich, M. Vogelsberger, and L. Hernquist, *Mon. Not. Roy. Astron. Soc.* **484**, 476 (2019), arXiv:1809.07255 [astro-ph.GA] .
- [27] J. Prada, J. E. Forero-Romero, R. J. J. Grand, R. Pakmor, and V. Springel, *Mon. Not. Roy. Astron. Soc.* **490**, 4877 (2019), arXiv:1910.04045 [astro-ph.GA] .
- [28] A. Lazar *et al.*, *Mon. Not. Roy. Astron. Soc.* **497**, 2393 (2020), arXiv:2004.10817 [astro-ph.GA] .
- [29] R. Dave, D. N. Spergel, P. J. Steinhardt, and B. D. Wandelt, *Astrophys. J.* **547**, 574 (2001), arXiv:astro-ph/0006218 .
- [30] A. Kusenko and P. J. Steinhardt, *Phys. Rev. Lett.* **87**, 141301 (2001), arXiv:astro-ph/0106008 .
- [31] R. N. Mohapatra, S. Nussinov, and V. L. Teplitz, *Phys. Rev. D* **66**, 063002 (2002), arXiv:hep-ph/0111381 .
- [32] S. W. Randall, M. Markevitch, D. Clowe, A. H. Gonzalez, and M. Bradac, *Astrophys. J.* **679**, 1173 (2008), arXiv:0704.0261 [astro-ph] .
- [33] N. Arkani-Hamed, D. P. Finkbeiner, T. R. Slatyer, and N. Weiner, *Phys. Rev. D* **79**, 015014 (2009), arXiv:0810.0713 [hep-ph] .
- [34] J. L. Feng, M. Kaplinghat, and H.-B. Yu, *Phys. Rev. Lett.* **104**, 151301 (2010), arXiv:0911.0422 [hep-ph] .
- [35] M. R. Buckley and P. J. Fox, *Phys. Rev. D* **81**, 083522 (2010), arXiv:0911.3898 [hep-ph] .
- [36] J. Koda and P. R. Shapiro, *Mon. Not. Roy. Astron. Soc.* **415**, 1125 (2011), arXiv:1101.3097 [astro-ph.CO] .
- [37] M. Vogelsberger, J. Zavala, and A. Loeb, *Mon. Not. Roy. Astron. Soc.* **423**, 3740 (2012), arXiv:1201.5892 [astro-ph.CO] .
- [38] C. Kouvaris, *Phys. Rev. Lett.* **108**, 191301 (2012), arXiv:1111.4364 [astro-ph.CO] .
- [39] S. Tulin, H.-B. Yu, and K. M. Zurek, *Phys. Rev. Lett.* **110**, 111301 (2013), arXiv:1210.0900 [hep-ph] .
- [40] S. Tulin, H.-B. Yu, and K. M. Zurek, *Phys. Rev. D* **87**, 115007 (2013), arXiv:1302.3898 [hep-ph] .
- [41] K. M. Zurek, *Phys. Rept.* **537**, 91 (2014), arXiv:1308.0338 [hep-ph] .
- [42] M. B. Wise and Y. Zhang, *Phys. Rev. D* **90**, 055030 (2014), [Erratum: *Phys. Rev. D* 91, 039907 (2015)], arXiv:1407.4121 [hep-ph] .
- [43] K. Petraki, L. Pearce, and A. Kusenko, *JCAP* **07**, 039, arXiv:1403.1077 [hep-ph] .
- [44] F. Kahlhoefer, K. Schmidt-Hoberg, M. T. Frandsen, and S. Sarkar, *Mon. Not. Roy. Astron. Soc.* **437**, 2865 (2014), arXiv:1308.3419 [astro-ph.CO] .
- [45] O. D. Elbert, J. S. Bullock, S. Garrison-Kimmel, M. Rocha, J. Oñorbe, and A. H. G. Peter, *Mon. Not. Roy. Astron. Soc.* **453**, 29 (2015), arXiv:1412.1477 [astro-ph.GA] .
- [46] M. Kaplinghat, S. Tulin, and H.-B. Yu, *Phys. Rev. Lett.* **116**, 041302 (2016), arXiv:1508.03339 [astro-ph.CO] .
- [47] K. Blum, R. Sato, and T. R. Slatyer, *JCAP* **06**, 021, arXiv:1603.01383 [hep-ph] .
- [48] P. Ullio and M. Valli, *JCAP* **07**, 025, arXiv:1603.07721 [astro-ph.GA] .
- [49] A. Kamada, M. Kaplinghat, A. B. Pace, and H.-B. Yu, *Phys. Rev. Lett.* **119**, 111102 (2017), arXiv:1611.02716 [astro-ph.GA] .
- [50] M. Battaglieri *et al.*, in *U.S. Cosmic Visions: New Ideas in Dark Matter* (2017) arXiv:1707.04591 [hep-ph] .
- [51] A. Robertson, R. Massey, and V. Eke, *Mon. Not. Roy. Astron. Soc.* **467**, 4719 (2017), arXiv:1612.03906 [astro-ph.CO] .
- [52] A. Robertson *et al.*, *Mon. Not. Roy. Astron. Soc.* **476**, L20 (2018), arXiv:1711.09096 [astro-ph.CO] .
- [53] S. Tulin and H.-B. Yu, *Phys. Rept.* **730**, 1 (2018), arXiv:1705.02358 [hep-ph] .
- [54] M. Valli and H.-B. Yu, *Nature Astron.* **2**, 907 (2018), arXiv:1711.03502 [astro-ph.GA] .
- [55] M. A. Buen-Abad, M. Schmaltz, J. Lesgourgues, and T. Brinckmann, *JCAP* **01**, 008, arXiv:1708.09406 [astro-ph.CO] .
- [56] A. Sokolenko, K. Bondarenko, T. Brinckmann, J. Zavala, M. Vogelsberger, T. Bringmann, and A. Boyarsky, *JCAP* **12**, 038, arXiv:1806.11539 [astro-ph.CO] .
- [57] M. Vogelsberger, J. Zavala, K. Schutz, and T. R. Slatyer, *Monthly Notices of the Royal Astronomical Society* **484**, 5437 (2019), <https://academic.oup.com/mnras/article-pdf/484/4/5437/27790344/stz340.pdf> .
- [58] A. Robertson, D. Harvey, R. Massey, V. Eke, I. G. McCarthy, M. Jauzac, B. Li, and J. Schaye, *Mon. Not. Roy. Astron. Soc.* **488**, 3646 (2019), arXiv:1810.05649 [astro-ph.CO] .
- [59] T. Ren, A. Kwa, M. Kaplinghat, and H.-B. Yu, *Phys. Rev. X* **9**, 031020 (2019), arXiv:1808.05695 [astro-ph.GA] .
- [60] R. Essig, S. D. McDermott, H.-B. Yu, and Y.-M. Zhong, *Phys. Rev. Lett.* **123**, 121102 (2019), arXiv:1809.01144 [hep-ph] .
- [61] E. O. Nadler, A. Banerjee, S. Adhikari, Y.-Y. Mao, and R. H. Wechsler, *Astrophys. J.* **896**, 112 (2020), arXiv:2001.08754 [astro-ph.CO] .
- [62] P. Agrawal, A. Parikh, and M. Reece, *JHEP* **10**, 191, arXiv:2003.00021 [hep-ph] .
- [63] K. Hayashi, M. Ibe, S. Kobayashi, Y. Nakayama, and S. Shirai, *Phys. Rev. D* **103**, 023017 (2021), arXiv:2008.02529 [astro-ph.CO] .
- [64] K. E. Andrade, J. Fuson, S. Gad-Nasr, D. Kong, Q. Minor, M. G. Roberts, and M. Kaplinghat, *Mon. Not. Roy. Astron. Soc.* **510**, 54 (2021), arXiv:2012.06611 [astro-ph.CO] .
- [65] K. Bondarenko, A. Sokolenko, A. Boyarsky, A. Robertson, D. Harvey, and Y. Revaz, *JCAP* **01**, 043, arXiv:2006.06623 [astro-ph.CO] .
- [66] D. Egana-Ugrinovic, R. Essig, D. Gift, and M. LoVerde, *JCAP* **05**, 013, arXiv:2102.06215 [astro-ph.CO] .
- [67] L. Sagunski, S. Gad-Nasr, B. Colquhoun, A. Robertson, and S. Tulin, *JCAP* **01**, 024, arXiv:2006.12515 [astro-ph.CO] .
- [68] B. Colquhoun, S. Heeba, F. Kahlhoefer, L. Sagunski, and S. Tulin, *Phys. Rev. D* **103**, 035006 (2021), arXiv:2011.04679 [hep-ph] .
- [69] T. Ebisu, T. Ishiyama, and K. Hayashi, *Phys. Rev. D* **105**, 023016 (2022), arXiv:2107.05967 [astro-ph.GA] .
- [70] M. S. Fischer, M. Brüggen, K. Schmidt-Hoberg, K. Dolag, A. Ragagnin, and A. Robertson, *Mon. Not. Roy. Astron. Soc.* **510**, 4080 (2022), arXiv:2109.10035 [astro-ph.CO] .
- [71] A. Zentner, S. Dandavate, O. Slone, and M. Lisanti, (2022), arXiv:2202.00012 [astro-ph.GA] .

- [72] M. Silverman, J. S. Bullock, M. Kaplinghat, V. H. Robles, and M. Valli, (2022), [arXiv:2203.10104 \[astro-ph.GA\]](#) .
- [73] D. Eckert, S. Etori, A. Robertson, R. Massey, E. Pointecouteau, D. Harvey, and I. G. McCarthy, (2022), [arXiv:2205.01123 \[astro-ph.CO\]](#) .
- [74] M. S. Fischer, M. Brüggen, K. Schmidt-Hoberg, K. Dolag, F. Kahlhoefer, A. Ragagnin, and A. Robertson, (2022), [arXiv:2205.02243 \[astro-ph.CO\]](#) .
- [75] B. Carr, K. Kohri, Y. Sendouda, and J. Yokoyama, *Rept. Prog. Phys.* **84**, 116902 (2021), [arXiv:2002.12778 \[astro-ph.CO\]](#) .
- [76] R. N. Mohapatra and S. Nussinov, *Phys. Lett. B* **776**, 22 (2018), [arXiv:1709.01637 \[hep-ph\]](#) .
- [77] E. Michaely, I. Goldman, and S. Nussinov, *Phys. Rev. D* **101**, 123006 (2020), [arXiv:1905.12643 \[astro-ph.HE\]](#) .
- [78] P. Bode, J. P. Ostriker, and N. Turok, *Astrophys. J.* **556**, 93 (2001), [arXiv:astro-ph/0010389](#) .
- [79] T. Asaka, M. Shaposhnikov, and A. Kusenko, *Phys. Lett. B* **638**, 401 (2006), [arXiv:hep-ph/0602150](#) .
- [80] M. Drewes *et al.*, *JCAP* **01**, 025, [arXiv:1602.04816 \[hep-ph\]](#) .
- [81] O. Newton, M. Leo, M. Cautun, A. Jenkins, C. S. Frenk, M. R. Lovell, J. C. Helly, A. J. Benson, and S. Cole, *JCAP* **08**, 062, [arXiv:2011.08865 \[astro-ph.CO\]](#) .
- [82] L. Hui, J. P. Ostriker, S. Tremaine, and E. Witten, *Phys. Rev. D* **95**, 043541 (2017), [arXiv:1610.08297 \[astro-ph.CO\]](#) .
- [83] C. B. Adams *et al.*, in *2022 Snowmass Summer Study* (2022) [arXiv:2203.14923 \[hep-ex\]](#) .
- [84] S. Girmohanta, R. N. Mohapatra, and R. Shrock, *Phys. Rev. D* **103**, 015021 (2021), [arXiv:2011.01237 \[hep-ph\]](#) .
- [85] S. Girmohanta and R. Shrock, *Phys. Rev. D* **104**, 115021 (2021), [arXiv:2109.02670 \[hep-ph\]](#) .
- [86] D. Kazanas, R. N. Mohapatra, S. Nussinov, V. L. Teplitz, and Y. Zhang, *Nucl. Phys. B* **890**, 17 (2014), [arXiv:1410.0221 \[hep-ph\]](#) .
- [87] A. Filippi and M. De Napoli, *Rev. Phys.* **5**, 100042 (2020), [arXiv:2006.04640 \[hep-ph\]](#) .
- [88] M. Fabbrichesi, E. Gabrielli, and G. Lanfranchi [10.1007/978-3-030-62519-1](#) (2020), [arXiv:2005.01515 \[hep-ph\]](#) .
- [89] P. S. Krstić and D. R. Schultz, *Phys. Rev. A* **60**, 2118 (1999).
- [90] F. A. Roper, K. A. Oman, C. S. Frenk, A. Benítez-Llambay, J. F. Navarro, and I. M. E. Santos-Santos, (2022), [arXiv:2203.16652 \[astro-ph.GA\]](#) .
- [91] E. Merzbacher, *Quantum Mechanics*, Wiley, New York (pp. 230-231) (1970).
- [92] M. Goldberger and K. M. Watson, *Collision Theory*, Wiley, New York (1964).